

MODELS FOR ZERO-TEMPERATURE STARS*

T. HAMADA

School of Physics, University of Sydney, N.S.W.

AND

E. E. SALPETER

Laboratory of Nuclear Studies and Center for Radiophysics and Space Research, Cornell University,
Ithaca, N.Y.; School of Physics, Sydney University, Sydney, N.S.W.;
Churchill College, Cambridge, England†*Received June 24, 1961*

ABSTRACT

The equation of state derived in the preceding paper is applied to models for zero-temperature stars. Models are evaluated numerically for stars consisting of He^4 , C^{12} , Mg^{24} , Si^{28} , S^{32} , or Fe^{56} . For the same central density, ρ_c , our models have smaller values of radius R and mass M than the simpler Chandrasekhar models. These deviations are most marked at the lowest densities (of order 20 per cent for $\rho_c \sim 10^5 \text{ gm/cc}$, $M \sim 0.1 M_\odot$).

For models with high density the most important effects are due to inverse beta decays in the interior of the star. Instead of the Chandrasekhar limiting mass ($1.46 M_\odot$ for He^4) as $\rho_c \rightarrow \infty$, one obtains a maximum value of mass M for a finite value of ρ_c . The value of this maximum mass depends on initial chemical composition. The lowest possible value is $1.01 M_\odot$ for the optimum chemical composition, the value of this maximum mass for Fe^{56} is $1.11 M_\odot$ and is largest for C^{12} ($1.40 M_\odot$). The values of ρ_c for the maximum mass are in the range 10^9 – 10^{10} gm/cc .

Models are constructed for zero-temperature stars which contain a hydrogen envelope. The presence of such an envelope increases the radius of the star but has little effect on the mass. For the more massive stars ($M \gtrsim 0.7 M_\odot$), only small hydrogen envelopes are possible.

Models are constructed for neutron stars ($\rho_c > 10^{13}$) containing a neutron core and an envelope consisting of electrons and ions. For $\rho_c < 3 \times 10^{14}$ the envelope contains most of the mass ($M > 0.5 M_\odot$). A sharp minimum mass of about $0.05 M_\odot$ is obtained at $\rho_c \sim 3.5 \times 10^{14}$, and for larger ρ_c the envelope is unimportant.

I. INTRODUCTION AND METHOD

Since the electrons in a white dwarf star are highly degenerate, theoretical studies of white dwarfs are based on the models of Chandrasekhar (1936, 1939) for zero-temperature stars. These models are based on the equation of state for a Fermi-Dirac gas of non-interacting electrons with a fixed value of μ , the inverse of the number of electrons per unit atomic mass.¹ In reality, electrostatic interactions between electrons and nuclei are of some importance at low densities, and inverse beta decays alter the value of μ at high densities. The main aim of the present paper is to correct the models of Chandrasekhar for these effects. Some such corrections have been calculated previously (see Schatzman 1958; Auluck and Mathur 1959), but the present work is based on a somewhat more accurate equation of state derived in a preceding paper (Salpeter 1961), hereafter referred to as "Paper I."

Let Z be the nuclear charge, A the atomic weight (of the neutral atom) in physical atomic mass units $M_u = 1.6604 \times 10^{-24} \text{ gm}$ and $\mu \equiv A/Z$ (so that $\mu = 2$ for O^{16}). Let x be the "relativity parameter," the ratio of Fermi momentum of the electrons to mc (m is the electron mass), so that the density ρ is given by

$$\rho = \frac{\mu M_u}{3\pi^2} \left(\frac{mc}{\hbar} \right)^3 x^3 = (\mu x^3) \times 9.738 \times 10^5 \text{ gm/cc}. \quad (1)$$

* Supported in part by a joint contract of the U.S. Atomic Energy Commission and the Office of Naval Research.

† Permanent address: Cornell University.

¹ The quantity is normally denoted by μ_e , but we drop the subscript.

We shall neglect corrections for general relativity throughout this paper, so that the equations of hydrostatic equilibrium are simply

$$\frac{dM(r)}{dr} = 4\pi r^2 \rho(r); \quad \frac{dP(r)}{dr} = -\frac{GM(r)}{r^2} \rho(r), \quad (2)$$

where $M(r)$ is the interior mass at radial distance r and P is the pressure.

In equation (2) we express the density ρ in terms of the parameter x by means of equation (1). For the equation of state we use equations (16)–(19) of Paper I, which express the total pressure P in terms of the parameter x (and the nuclear charge Z). For a given chemical composition and density (value x_c of x) at the center [$r=0$ with $M(0)=0$] one simply integrates equation (2) outward. As discussed in Paper I, our equation of state would lead to negative pressures at very low densities. The outward integration was stopped at that value R of the radial distance r for which our formulae give zero pressure. For stellar masses $M \gtrsim 0.2 M_\odot$ the error in the stellar radius R due to the neglect of the outermost low-density regions should be very small. For central densities ρ_c less than about 10^{10} gm/cc, corrections due to general relativity are also small.

Since our equation of state depends on the atomic charge Z , as well as on x , separate numerical calculations have to be performed for different chemical compositions, as well as for different values of the central density ρ_c . The second equation in equation (2) was transformed into an equation for $dx(r)/dr$ with the help of the equation of state. The numerical integrations were carried out by the Kutta-Gill method (Gill 1951) on the Silliac computer at the University of Sydney. Unless stated otherwise, the purely numerical errors in the tables presented below should be less than about 0.2 per cent for the stellar radius R and appreciable smaller still for the stellar mass M . In models with a discontinuity in chemical composition, the pressure was taken as continuous across the boundary, so that the density has a discontinuity.

In Section II we discuss restrictions on the chemical composition which can be present in cooled-down white dwarfs. Some of these restrictions come simply from the pycnonuclear reactions and inverse beta decays, discussed in Paper I, which could proceed even at zero temperature. In particular, this leads to upper limits on the size of hydrogen envelopes which zero-temperature stars of different masses can have. Some additional restrictions come from estimates on earlier stages of evolution when the star was hot enough to undergo thermonuclear reactions. In particular, this leads to estimates for stellar masses above which a cool white dwarf cannot contain very much helium.

In Section III the main results of the numerical model calculations are presented. For convenience we also give values of μ_{eff} , the fictitious value of μ for which a Chandrasekhar model would give the mass and radius as some of our models. The corrections due to Coulomb effects are strongest at low densities (small masses), and the maximum radius of cold objects is discussed. The inverse beta decays lead to a maximum mass at finite central density, instead of Chandrasekhar's limiting mass. The main purpose of this paper is the evaluation of this maximum mass for various initial chemical compositions.

In Section IV we present the results for models with an envelope consisting of hydrogen (or helium), and in Section V for stars at very high densities which consist mainly of neutrons in their deep interior. In Section V we also discuss briefly the possible relation of neutron stars to remnants of supernovae explosions.

II. RESTRICTIONS ON CHEMICAL COMPOSITION

In Section V of Paper I we discussed restrictions on the values of Z and A which can be maintained over appreciable periods of time at high densities. Pycnonuclear reactions lead to the instability of H^1 (change to He^4) at densities ρ much greater than

about 5×10^4 gm/cc, of He^4 (change to C^{12}) at $\rho > 8 \times 10^8$ gm/cc and of C^{12} (change to Mg^{24}) at $\rho > 6 \times 10^9$ gm/cc. The numerical values of these critical densities should be reliable to within a factor of about 3 or 4. For Mg^{24} and heavier nuclei the critical densities beyond which they will suffer inverse beta decays are given in Table 1 of Paper I. We have carried out stellar integrations for uniform composition for models where ρ_c is less than the appropriate critical density. For other models we have introduced discontinuities in chemical composition at radial distances such that the density at the outside of the discontinuity equals the critical density. Since we are mainly interested in models with $\rho_c > 10^5$ gm/cc, we have not considered any models with hydrogen in the central regions.

We have taken into account explicitly in our models only those restrictions on chemical composition that are required for a star at zero temperature irrespective of its previous history. In reality, a star will have encountered more severe restrictions at earlier phases of its evolution. If a star evolves at constant mass M , its central temperature will reach a maximum T_m at some stage where the electrons in its interior are partially degenerate. Those nuclear species that "burn" rapidly at temperatures near T_m and lower will then be missing also when the star has finally cooled down. T_m is an increasing function of stellar mass M , and, if a star loses mass in its late evolutionary phases, the actual maximum temperature reached will have been even higher than the value of T_m appropriate to the final mass M of the zero-temperature star. We assume the absence of any increase in mass due to accretion or capture from a companion star, so that T_m gives a lower limit to the maximum temperature that a zero-temperature star of final mass M had reached in earlier phases of evolution.

He^4 is transformed rapidly to C^{12} at temperatures of about 1.5×10^8 °K. According to Cox (1961), the electrons in the interior of a helium-burning star of mass $0.5 M_\odot$ (central temperature 1.25×10^8 °K) are still fairly non-degenerate; consequently, we have $T_m > 1.25 \times 10^8$ °K. According to Aller (1959), T_m is less than the temperature required for helium-burning for mass appreciably less than $0.5 M_\odot$. If we make the rather *ad hoc* assumption that kT_m is of the order of $0.1E_F$, where E_F is the Fermi energy at the center of the zero-temperature star with mass M , we find $T_m \sim 1.7 \times 10^8$ °K for $M = 0.5 M_\odot$, in qualitative agreement with the arguments above. We conclude that a zero-temperature star with $M > 0.5 M_\odot$ must have burned at an earlier stage an appreciable fraction of any helium originally contained in its interior. For $M \gtrsim 0.75 M_\odot$, we therefore consider only models with C^{12} or heavier atoms in the central regions of the star. Stars containing He^4 in the outermost layers are considered in Section IV. Note that even a zero-temperature star with $M = 0.75 M_\odot$ has values of ρ_c below 10^7 gm/cc for which pycnonuclear reactions involving He^4 at zero temperature are extremely slow, so that no helium-burning is of any importance after the star has started to cool down.

We need not consider stars with hydrogen in their interior but have to estimate the maximum amount of hydrogen that could be present in the outer layers. If there is a hydrogen envelope in the zero-temperature star starting at radial distance r , r must certainly be sufficiently large that $\rho(r) \lesssim 5 \times 10^4$ gm/cc. In fact, however, any hydrogen envelope present originally must have been burned into helium out to even greater radial distances at earlier, hotter, stages of evolution. Consider, for example, a stage in the cooling process where kT was about $0.05E_F$ at a radial distance r where $\rho(r) = 5 \times 10^4$ gm/cc. This gives $T \approx 1.3 \times 10^7$ °K, at which temperature hydrogen burns very much more rapidly (at fixed density) than at zero temperature. On the other hand, $kT/E_F \sim 0.05$ is sufficiently small for the density $\rho(r)$ to have been affected little by the non-zero temperature. Very little hydrogen could then have survived to the zero-temperature stage at layers where $\rho(r) \sim 5 \times 10^4$ gm/cc. This argument is based on current estimates for the pycnonuclear conversion rates of hydrogen into helium, which,

unfortunately, are not very accurate. It is hoped that more accurate calculations will confirm our conclusion.

For the burning of C^{12} and heavier nuclei, temperatures T of about 10^9 ° K are required, and at these high temperatures neutrino energy-loss processes are important. For $T \lesssim 5 \times 10^9$ ° K the reaction times for these neutrino processes are still appreciably longer than gravitational free-fall times for a star. One would then expect the maximum temperature T_m during earlier stages of evolution to be little affected by the neutrino processes. On the other hand, the neutrino energy loss per second is appreciably higher than the luminosity, and the detailed structure of such stars is not known at the moment. In view of this uncertainty, we consider zero-temperature stars containing C^{12} , Mg^{24} , Si^{28} , or S^{32} , as well as stars containing Fe^{56} .

III. THE MAIN RESULTS

The results for mass M and radius R for various central densities ρ_c and different chemical compositions are presented in Tables 1-4. In Table 1 the entries under R_{Ch}

TABLE 1A*

ZERO-TEMPERATURE MODELS FOR VARIOUS VALUES OF CENTRAL DENSITY, ρ_c (in gm/cc)

	LOG ρ_c							
	5 086	5 387	5 738	6 026	6 290	6 554	6 842	7 193
R_{Ch}	2 273	2 018	1 753	1 558	1 394	1 244	1 094	0 930
M_{Ch}	0 164	0 224	0 316	0 411	0 512	0 622	0 748	0 899
R_{He}	2 181	1 952	1 708	1 524	1 368	1 224	1 079	0 919
M_{He}	0 154	0 213	0 305	0 399	0 499	0 609	0 734	0 885
$\mu_{eff, He}$	2 07 ₅	2 05 ₅	2 04	2 03 ₅	2 03	2 02 ₅	2 02	2 01 ₅
R_C	2 111				1 348	1 208	1 067	0 910
M_C	0 147				0 488	0 597	0 722	0 872
$\mu_{eff, C}$	2 13				2.06	2 05	2 04	2 03 ₅
R_{Mg}	2 032	1 844	1 632	1 468	1 325	1 191	1 054	0 900
M_{Mg}	0 139	0 196	0 286	0 378	0 476	0 584	0 708	0 857
$\mu_{eff, Mg} \dots$	2 21	2 17	2 13	2 11	2 09	2 07	2 06	2 05

* Radii R are in units of $0.01R_\odot$, masses M in units of M_\odot

TABLE 1B*

	LOG ρ_c							
	7 721	8 208	8 825	9.283	9 499	9 778	10 000	10.400
R_{Ch}	0 718	0 556	0 393	0 299	0 261	0 219	0 189	0 145
M_{Ch}	1 097	1 235	1 347	1 396	1 411	1 426	1 434	1 444
R_C	0 706	0 548	0 388	0 296	0 258	0 216*	0 208	0 170
M_C	1 070	1 206	1 318	1 366	1 381	1 396*	1 349	1 174
R_{Mg}	0 699	0 544	0 386	0 294	0 257*	0 243	0 216	
$M_{Mg} \dots$	1 053	1 190	1 300	1 348	1 363*	1 282	1 205	

* Models marked with an asterisk have central densities at which inverse beta decays are on the verge of occurring

TABLE 2*
MODELS FOR ZERO-TEMPERATURE STARS COMPOSED OF Fe⁵⁶

	LOG ρ_c				
	3 50	3 85	3 94	4 09	4 50
R_{Fe}	2 015	2 102	2 105	2 096	2 004
M_{Fe}	0 007	0 015	0 018	0 024	0 046

	LOG ρ_c							
	5 086	5 387	5 738	6 026	6 290	6 554	6 842	7 193
R_{Ch}	2 138	1 899	1 650	1 466	1 313	1 171	1 031	0 877
M_{Ch}	0 136	0 187	0 265	0 345	0 430	0 525	0 633	0 765
R_{Fe}	1 772	1 632	1 464	1 328	1 206	1 089	0 968	0 830
M_{Fe}	0 103	0 149	0 222	0 298	0 380	0 471	0 576	0 703
$\mu_{\text{eff, Fe}}$	2 53	2 46	2 39	2 35	2 32	2 29	2 27	2 25 ₅

	LOG ρ_c							
	7 721	8 208	8 825	9 060	9 290	9 885	10 390	10 588
R_{Fe}	0 648	0 506	0 359	0 314*	0 286	0 197	0 138*	0 127
M_{Fe}	0 872	0 991	1 088	1 112*	1 093	1 028	1 014*	0 990

* ρ_c is central density in gm/cc, R is radius in units of $0.01R_{\odot}$, M is mass in units of M_{\odot}

TABLE 3*
ZERO-TEMPERATURE MODELS FOR Si²⁸ AND S³²

	LOG ρ_c							
	Si ²⁸			S ³²				
	9 028	9 290	9 855	7 623	8 162	9 086	10 68	10 85
R	0 342	0 292*	0 230	0 730	0 555*	0 346	0 112*	0 108
M	1 319	1 343*	1 175	1 011	1 169*	1 064	1 067*	1 047

* ρ_c in gm/cc, R in units of $0.01R_{\odot}$, M in units of M_{\odot}

and M_{Ch} denote the radius and mass in the Chandrasekhar approximation for $\mu = A/Z = 2$. The other entries are results using our improved equation of state for He^4 ($\mu = 2.002$), C^{12} ($\mu = 2.001$), and Mg^{24} ($\mu = 1.999$). The entries marked with an asterisk have the highest central densities at which C^{12} or Mg^{24} is stable; later entries refer to models with a core of Ne^{24} and an outer zone of C^{12} and Mg^{24} , respectively. Table 2 gives the results for ${}^{56}_{26}\text{Fe}$ ($\mu = 2.152$), together with the Chandrasekhar ap-

TABLE 4*
ZERO-TEMPERATURE MODELS FOR EQUILIBRIUM COMPOSITION

	LOG ρ_c							
	8 627	8 920	9 147	9 361	9 692	10 28	11 28	11 53
(Z; A)	28; 62	28; 64	28; 64	28; 66	28; 66	30; 78	32; 90	38; 120
R.	0 400	0 343	0 300	0 267	0 216	0 157	0 080	0 074
M .	1 000	1 011	1 015	1 005	0 990	0 913	0 753	0 711

* (Z; A) denotes the nuclear species at the center (ρ_c in gm/cc, R in units of $0.01R_\odot$, M in units of M_\odot)

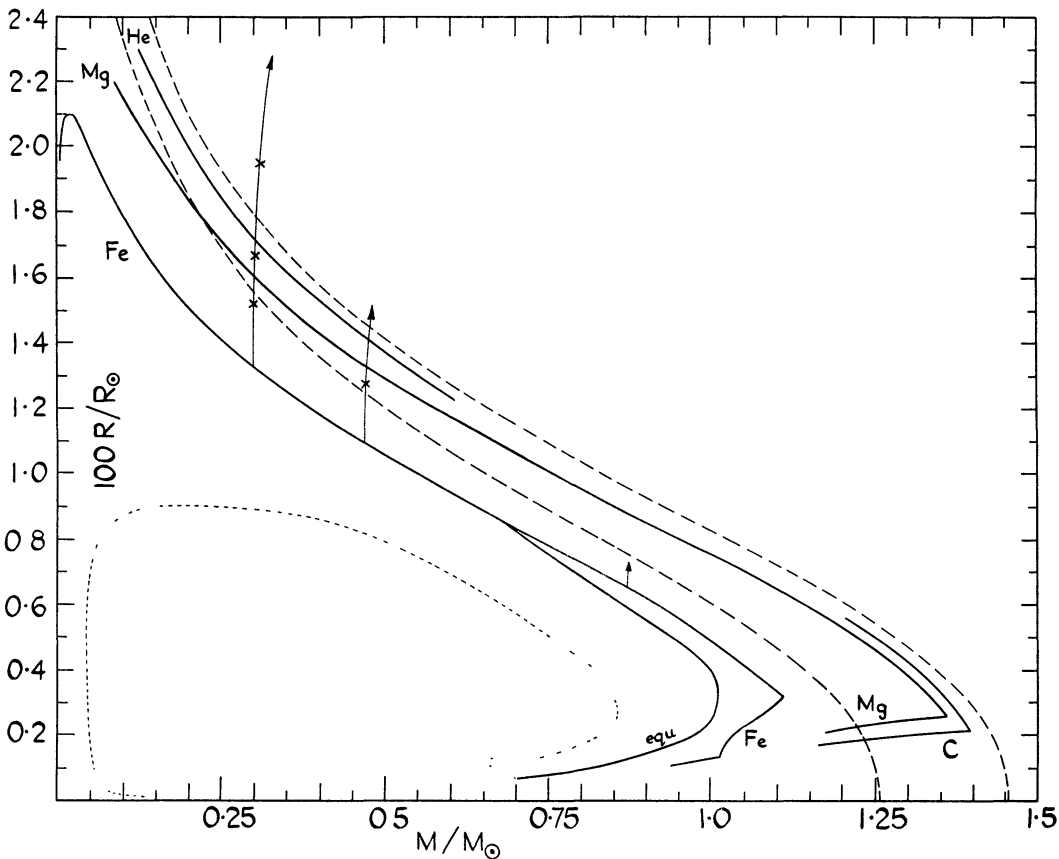


FIG. 1.—The relation between mass M and radius R for zero-temperature stars for He^4 , C^{12} , Mg^{24} , and Fe^{56} . The curve marked *equ* denotes equilibrium composition at each density. The dashed curves denote the Chandrasekhar models, the upper one for $\mu = 2$ and the lower one for $\mu = 2.15$. The dotted curves denote neutron stars. The vertical arrows denote stars with H^1 in the outer layers.

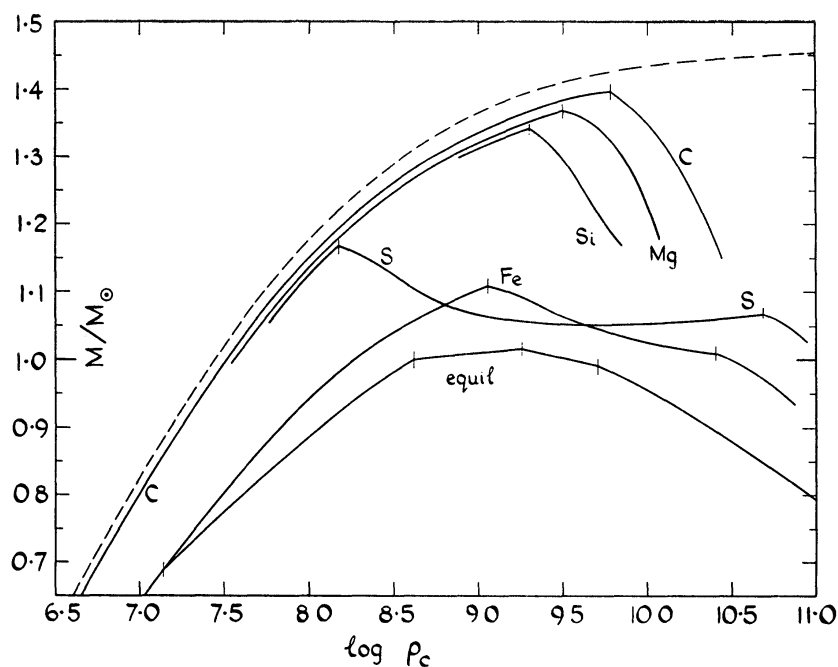


FIG. 2.—The relation between mass M and central density ρ_c (in gm/cc) for zero-temperature stars He^4 , C^{12} , Mg^{24} , Si^{28} , S^{32} , and Fe^{56} and for equilibrium conditions.

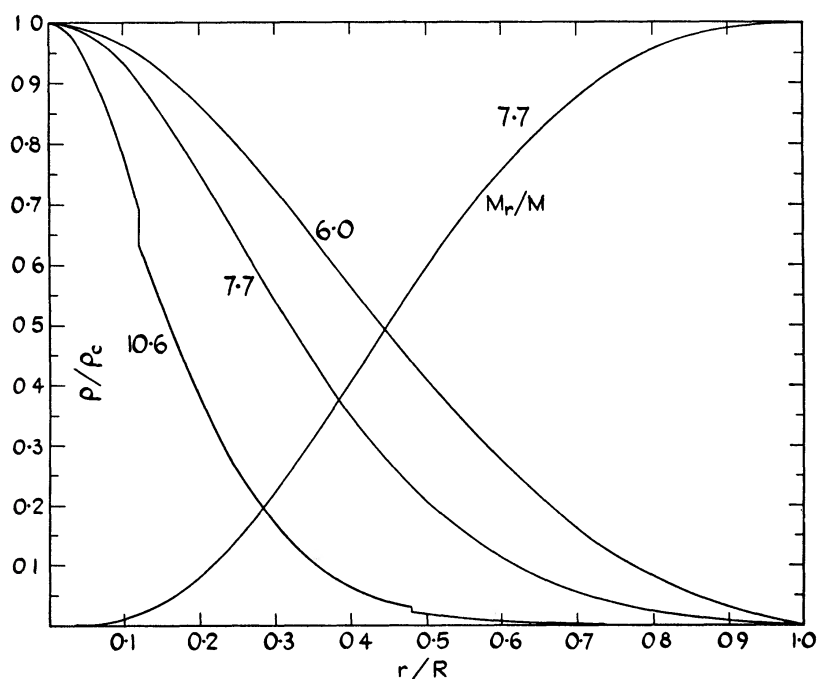


FIG. 3.—Density ρ as a function of radial distance r (in units of central density ρ_c and radius R , respectively) for Fe^{56} . The curves are labeled by the value of $\log \rho_c$ (in gm/cc). The curve labeled M_r/M denotes the fractional mass inside a sphere of radius r .

proximation for this value of μ . The two entries beyond the first asterisk refer to models which contain ${}^{24}\text{Cr}^{56}$, and the last entry ${}^{22}\text{Ti}^{56}$, in the center. Similarly, Table 3 gives results for Si^{28} and S^{32} (see Table 1 of Paper I for the transformed nuclear species at higher density). The mass-radius relations are also plotted in Figure 1 and the mass-central-density relations in Figure 2.

To each point in the M - R plane there corresponds one Chandrasekhar model with unique values for μ and ρ_c . In Tables 1 and 2 we also give μ_{eff} , the value of μ of that Chandrasekhar model that gives the same values of M and R as our more accurate models. μ_{eff} is seen to be a slowly varying function of ρ_c (for the homogeneous models), and interpolation may be used. One should remember, however, that the values of ρ_c for our actual model differ slightly from those for the Chandrasekhar model with the same M and R . The values of $\rho(r)/\rho_c$ as functions of r/R are shown for our homogeneous Fe models with $\rho_c = 6.03$ and 7.72 in Figure 3. The shapes of these curves are qualitatively similar to, but not identical with, those of the corresponding Chandrasekhar models. The shapes can be parametrized by the values of the ratio $\rho_c/\bar{\rho}$, where $\bar{\rho}$ is the average density of the whole star. For the Chandrasekhar models $\rho_c/\bar{\rho}$ varies from 5.99 for $\rho_c = 0$ to 54.18 for $\rho_c = \infty$ and $\rho_c/\bar{\rho} \approx 6.4, 7.1$, and 13.3 for $\log \rho_c = 5.09, 6.03$, and 7.72 , respectively. For our models $\rho_c/\bar{\rho} \approx 4.8, 6.0$, and 11.9 for $\log \rho_c = 5.09, 6.03$, and 7.72 , respectively (all for Fe^{56}).

For a homogeneous model with x_c , the central value of the relativity parameter in equation (1), very much larger than unity, our models bear a simpler relation to the Chandrasekhar models. According to equation (20) of Paper I, the ratio P/P_0 of actual to approximate pressure tends toward a constant limit in the extreme relativistic region $x \rightarrow \infty$. If ρ_c is sufficiently large that $x \gg 1$, throughout most of the star, our homogeneous model will have the same $\rho(r)$, M , and R as a Chandrasekhar model with

$$\mu_{\text{eff}} = \mu \left(\frac{P}{P_0} \right)^{-0.75}. \quad (3)$$

This limiting expression gives $\mu_{\text{eff, He}} = 2.011$, $\mu_{\text{eff, C}} = 2.021$, $\mu_{\text{eff, Mg}} = 2.034$, and $\mu_{\text{eff, Fe}} = 2.217$. For $\log \rho_c = 7.72$ and 8.83 , respectively, a comparison of the actual numerical models gives $\mu_{\text{eff, Mg}} \approx 2.045, 2.035$, and $\mu_{\text{eff, Fe}} \approx 2.24, 2.22$. Our actual models with very large values of ρ_c have discontinuities in chemical composition and hence in $\rho(r)$. In Figure 3 the function $\rho(r)/\rho_c$ is shown for a model with $\log \rho_c = 10.59$ containing ${}^{22}\text{Ti}^{56}$, ${}^{24}\text{Cr}^{56}$, and ${}^{26}\text{Fe}^{56}$ in the inner, middle, and outer regions. The value of $\rho_c/\bar{\rho}$ is about 57 for this model, compared with about 42 for a homogeneous Chandrasekhar model with the same value of ρ_c .

For the homogeneous models ($\rho_c < 10^9$), those with the lowest values of the central density ρ_c (and the largest value of the atomic charge Z) differ most strongly in their values for M and R from the corresponding Chandrasekhar models. For applications to white dwarfs, only models with $\rho_c \gtrsim 10^5$ and $Z \leq 26$ are of interest. For these models equation of state of Paper I, which we have used throughout, should be a good approximation. For $Z = 26$, for instance, the two K-shell electrons would be bound to the nucleus with a K-shell density greater than the average electron density (an effect which we neglect) only for densities less than about 2.5×10^4 gm/cc. Singh (1957) obtained much smaller deviations from the Chandrasekhar models than ours, but his results are incorrect, especially for large Z . He treated the ions as a continuous distribution of charge which would be a good approximation only for $Z \ll 1$. For $Z \geq 1$ the most important effects are missing in Singh's treatment.²

² The first paragraph in Sec. 3 of Singh and Noel (1960) is also incorrect (except for $Z \ll 1$). As discussed in Paper I, the screening of the ions by electrons becomes effective only at densities much lower than those found in white dwarfs.

a) *Maximum Radius*

For still lower values of ρ_c the deviations from the Chandrasekhar models become more marked, and the radius R of a cold body does not keep on increasing with decreasing mass M (i.e., decreasing ρ_c). The maximum radius for a cold body and the corresponding mass have been estimated by Kothari (1938). The equation of state of Paper I also leads to a maximum radius as a function of ρ_c , and models for Fe^{56} near this maximum radius are given at the beginning of Table 2. The maximum radius obtained is about $0.021 R_\odot$, with a mass of about $0.02 M_\odot$. We have not evaluated numerical models for values of the atomic charge other than 26 (and $\mu = 2.15$). Very roughly, however, the maximum radius should be proportional to $(\mu Z)^{-1/3}$ and the corresponding mass to Z/μ^2 .

Our model with the maximum radius for $Z = 26$ has $\rho_c \sim 10^4$ gm/cc, only about 30 times the density at which our equation of state leads (incorrectly) to zero pressure. Our models are not very reliable in this density range, where the atomic K shell (and part of the L shell) are intact and effectively screen the nucleus. A better approximation would be obtained from our equation of state by substituting $Z'(\rho) = Z - s(\rho)$ for Z and $\mu'(\rho) = A/Z'$ for μ , where $s(\rho)$ is a density-dependent screening parameter. In such an improved treatment the radius R would presumably have a broader maximum as a function of mass M , and the value of M for the maximum R would probably be appreciably smaller.³

b) *The Chandrasekhar Limit*

For Chandrasekhar models with homogeneous chemical composition, the stellar mass is a monotonically increasing function of density ρ_c and tends to a finite limiting mass M_l as $\rho_c \rightarrow \infty$. With $\mu = A/Z$ and A in physical atomic-mass units ($\mu = 2$ for O^{16} and $\mu = 1.008$ for H^1), we have

$$M_l = \left(\frac{2}{\mu}\right)^2 1.4587 M_\odot. \quad (4)$$

With our equation of state, but still for homogeneous models, one would obtain a limiting mass given by the same expression but with μ replaced by the constant μ_{eff} given in equation (3). In fact, however, inverse beta decays result in central regions of the star with lower values of μ . As a consequence, the mass M as a function of ρ_c reaches a maximum value M_{max} for some large, but finite, value of ρ_c , and M decreases for still larger values of ρ_c . The maximum mass M_{max} was estimated approximately by Schatzman (1958), but our stellar models give more accurate values for M_{max} , separately for each chemical composition assumed to be present before the nuclear transformations.

The results for C^{12} , Mg^{24} , Si^{28} , D^{32} , and Fe^{56} are displayed in Figure 2. In all five cases the maximum mass is reached for the largest value of ρ_c for which a homogeneous model is possible, with $M_{\text{max}} \approx 1.396, 1.36, 1.34, 1.17$, and 1.11 , respectively (in units of M_\odot). We also have a series of models for "equilibrium chemical composition," where both Z and A are assumed to have the optimum value for the density at each point in the star. The composition at various densities is taken from Table 2 of Paper I and the models are given in Table 4 of the present paper. For this series we have $M_{\text{max}} \approx 1.015 M_\odot$.

Our range of values of M_{max} from about $1.01 M_\odot$ to $1.40 M_\odot$ has the following evolutionary significance: (1) A star with $M < 1.01 M_\odot$, irrespective of previous history and chemical composition, cannot contract beyond a critical finite central density of the order of 10^9 gm/cc or less (assuming the absence of a subsequent mass increase by accretion or capture from a companion star). (2) A star with $M > 1.40 M_\odot$, irrespective of previous history and chemical composition, must contract to central densities appreci-

³ At still lower densities our unmodified equation of state would lead to completely unreliable models and would not be applicable to planets.

ably exceeding 10^{10} gm/cc as soon as its nuclear fuel has been exhausted (assuming the absence of angular momentum, a magnetic field, and subsequent mass loss). (3) The appreciable range of stellar masses in between 1.01 and $1.40 M_{\odot}$ may be of significance in connection with the theory of Hoyle and Fowler (1960) for the formation of supernovae of type I. This theory requires a pre-supernova star of very high central density but relatively low temperature. According to the Chandrasekhar models, this condition could be achieved only by a star of mass just slightly larger than the limiting mass M_L . According to our models, a star with mass in the range from $1.01 M_{\odot}$ to slightly larger than $1.40 M_{\odot}$ might do. For instance, a star originally composed of Mg^{24} with $M \approx 1.2 M_{\odot}$ would contract to central densities of about 10^8 gm/cc at relatively low temperatures, but the densities and temperatures might nevertheless be sufficiently high for an appreciable fraction of the Mg to be transformed into Fe, say. After this conversion the stellar mass would exceed the new value of $M_{\max} \approx 1.11 M_{\odot}$, and further contraction can take place. This particular conjecture must, of course, be tested by carrying out actual evolutionary stellar models based on detailed estimates for the rates of thermonuclear reactions. It is hoped that the present series of zero-temperature static models will be useful as a background for such evolutionary models.

IV. ENVELOPES CONTAINING HYDROGEN

We have considered so far only models which are homogeneous except for changes in chemical composition in the interior of the star necessitated by inverse beta decays and pycnonuclear reactions. We now consider models with an envelope consisting of lighter atoms, in particular hydrogen.

Results for these inhomogeneous models are presented in Tables 5–7. Table 5 refers to stars consisting of Fe^{56} with an envelope consisting of H^1 . In the numerical calculations the pressure was assumed to be continuous across the Fe-H boundary, so that the density has a discontinuity. ρ_H denotes the density on the hydrogen (outer) side of the boundary, M_H/M is the fraction of the total mass contained in the hydrogen envelope. Radius R and mass M are given for three series of models with three different values of the central density ρ_c . It may be of some interest to compare an inhomogeneous model with a homogeneous one containing a uniform mixture of Fe and H in the same proportions. The value of μ for such a homogeneous star would be given by

$$\mu_{av} = \left[\mu_{Fe}^{-1} + (\mu_H^{-1} - \mu_{Fe}^{-1}) \frac{M_H}{M} \right]^{-1}, \quad (5)$$

where $\mu_{Fe} = 2.152$ and $\mu_H = 1.008$. As discussed in the previous section, for any pair of values of R and M for our inhomogeneous models one can find values of μ_{eff} and ρ_c for which a Chandrasekhar model gives the same values of R and M . Table 5 also gives μ_{av} and μ_{eff} .

As the fraction of mass contained in the envelope is increased, the radius of the star increases considerably, whereas the mass increases very little. This effect was also present in inhomogeneous models obtained previously by Schatzman (1947). Furthermore, the increase in radius is more marked than it would be for a homogeneous model containing the same total fraction of hydrogen. This effect is qualitatively similar to (but weaker than) the effect of a hydrogen envelope on the radius of a red giant star or of a "helium-burning main-sequence" star (Cox and Salpeter 1961). The strength of the effect as a function of M_H/M does not depend very sensitively on the value of the central density ρ_c .

As discussed in Section II, hydrogen is converted fairly rapidly into helium at densities above about 5×10^4 gm/cc. Inhomogeneous models with $\log \rho_H > 4.7$ in Table 5 are therefore not likely to be encountered in nature. The three thin, almost vertical, lines in the M - R plot in Figure 1 represent our three series of inhomogeneous models.

The three crosses in the line on the left represent models with $M_{\text{H}}/M \approx 0.10, 0.03$, and 0.01 , respectively; the cross on the middle line represents $M_{\text{H}}/M = 0.01$. The arrowheads of the three lines represent models in which $\log \rho_{\text{H}} \approx 4.7$. For the more massive stars, with high central density, the maximum allowed hydrogen envelope is rather insignificant, but this is not the case for low-mass, low-density stars. As discussed in Section II, the maximum value of ρ_{H} should, in reality, be even lower than 5×10^4 gm/cc, since part of the hydrogen envelope must have been burned to helium at earlier evolutionary stages when the star was still hot. Nevertheless, hydrogen envelopes with an appreciable radius cannot be ruled out for white dwarfs of very low mass. Cox and Salpeter (1961) estimated that a hydrogen envelope of fractional mass $M_{\text{H}}/M \sim 0.1$ could survive in a helium-burning star and stars of mass appreciably less than about $0.3 M_{\odot}$ probably never could be hot enough to burn helium.

TABLE 5
MODELS WITH CORE OF Fe^{56} AND ENVELOPE OF H^1 WITH
DENSITY ρ_{H} AT BOUNDARY
 $\log \rho_{\text{c}} = 6.026$

	M_{H}/M					
	0	0.012	0.029	0.060	0.120	0.209
$\log \rho_{\text{H}}$	3.921	4.152	4.343	4.532	4.688
$100R/R_{\odot}$	1.328	1.549	1.659	1.801	2.018	2.279
M/M_{\odot}	0.298	0.299	0.300	0.303	0.313	0.331
μ_{av}	2.15	2.12	2.08	2.02	1.89	1.74
μ_{eff}	2.35	2.17	2.08	1.99	1.81	1.71

$\log \rho_{\text{c}} = 6.554$

	M_{H}/M			
	0	0.008	0.051	0.127
$\log \rho_{\text{H}}$. . .	4.265	4.761	5.015
$100R/R_{\odot}$	1.089	1.240	1.451	1.685
M/M_{\odot}	0.471	0.472	0.478	0.496
μ_{av}	2.15	2.13	2.03	1.88
μ_{eff}	2.29	2.16	2.00	1.83

$\log \rho_{\text{c}} = 7.721$

	M_{H}/M			
	0	0.0013	0.0133	0.0223
$\log \rho_{\text{H}}$. . .	4.648	5.290	5.441
$100R/R_{\odot}$	0.647	0.695	0.781	0.820
M/M_{\odot}	0.872	0.872	0.874	0.877
μ_{av}	2.15	2.15	2.12	2.10
μ_{eff}	2.24	2.20	2.13	2.10

TABLE 6
MODELS WITH CORE OF He⁴ AND ENVELOPE OF H¹ WITH DENSITY ρ_{H}
AT BOUNDARY AND LOG $\rho_c = 5.738$ AT CENTER

	M_{H}/M					
	0	0 024	0 053	0 143	0 264	0 440
$\log \rho_{\text{H}}$	3 882	4 106	4 385	4 570	4 747
$100R/R_{\odot}$	1 707	1 968	2 102	2 388	2 690	3 060
M/M_{\odot}	0 305	0 306	0 308	0 321	0 343	0 396

TABLE 7
MODELS WITH CORE Fe⁵⁶ AND ENVELOPE OF He⁴ WITH
DENSITY ρ_{He} AT BOUNDARY
log $\rho_c = 6.026$

	M_{He}/M					
	0	0 015	0 039	0 076	0 157	0 350
$\log \rho_{\text{He}}$	4 316	4 601	4 810	5 052	5 352
$100R/R_{\odot}$	1 328	1 376	1 393	1 411	1 438	1 484
M/M_{\odot}	0 298	0 298	0 299	0 299	0 301	0 309

log $\rho_c = 6.554$

	M_{He}/M			
	0	0 018	0 057	0 179
$\log \rho_{\text{He}}$	4 834	5 185	5 577
$100R/R_{\odot}$	1 089	1 124	1 141	1 171
M/M_{\odot}	0 471	0 471	0 472	0 477

log $\rho_c = 7.721$

	M_{He}/M			
	0	0 014	0 076	0 138
$\log \rho_{\text{He}}$	4 966	6 232	6 464
$100R/R_{\odot}$	0 657	0 655	0 679	0 689
M/M_{\odot}	0 872	0 872	0 875	0 879

Similar models are given in Table 6 for inhomogeneous stars containing He^4 in the interior with a hydrogen envelope. The results are very similar to the inhomogeneous models with Fe in their interior. Finally, results are given in Table 7 for models containing Fe in the interior with an envelope consisting of He^4 . The effect of the envelope (for a given fractional mass) on the radius is much less marked than that of a hydrogen envelope, since the values of μ vary rather little from He to Fe. In particular, these inhomogeneous models do not differ very markedly from homogeneous models containing uniform mixtures of Fe and He in the same proportions. More realistic models might contain successive layers of Fe, Mg, C, He, and an outer envelope of H, but only the discontinuity to the hydrogen layer is critical.

V. NEUTRON STARS

In Table 4 we have given models with "equilibrium chemical composition" for central densities ρ_c up to about 3.4×10^{11} gm/cc. As discussed in Paper I, some of the nuclei like ${}_{38}\text{Sr}^{120}$ dissolve into free neutrons at higher density. At these higher densities the Fermi energy of the electrons remains nearly constant, so that the partial density of ${}_{38}\text{Sr}^{120}$ remains at about 3.4×10^{11} and the partial pressure contributed by the electrons remains nearly constant.

For $\rho > 7 \times 10^{11}$ (in gm/cc) the partial density of free neutrons is then greater than the partial density of the ionized Sr. Because the neutron mass is much greater than the electron mass, the partial pressure of the neutrons is appreciably smaller than that of the electrons contributed by the ionized Sr when the two partial densities are the same ($\rho \sim 6.8 \times 10^{11}$). At densities much less than nuclear densities, the neutrons approximate a non-relativistic Fermi gas, and their partial pressure is roughly proportional to $(\rho - 3.4 \times 10^{11})^{5/3}$. At densities of $\rho \gtrsim 10^{13}$ the attractive nuclear forces give an appreciable negative contribution to the neutron pressure, and for $\rho > 10^{14}$ the repulsive core of the nuclear forces gives a positive contribution to the neutron pressure which increases very rapidly with increasing density. Cameron (1959) has developed a simple semiempirical formula for the neutron pressure as a function of the partial neutron density. This formula, while not very accurate, should be reasonably reliable in the density range $\rho \sim 10^{13}$ – 10^{16} (Salpeter 1960).

At a density of $\rho \sim 10^{13}$ the partial density and partial pressure of the ionized Sr plus electrons is only about 0.03 and 0.02, respectively, of the total. For central densities above 10^{13} , Cameron (1959) has carried out stellar-model integrations for zero-temperature neutron stars, using his formula for the neutron pressure and neglecting entirely the partial density and pressure of the ions and electrons. For $\rho_c < 10^{15}$, the effects of general relativity alter the radius and mass of a neutron star by less than 10 per cent. In the first two columns of Table 8 we give the radius R_m and mass M_n of models obtained by Cameron's method, but with general relativity neglected. We have also carried out models (also without general relativity) in which we take the ions and electrons into account. These models have a core with neutrons at partial density $(\rho - 3.4 \times 10^{11})$ and a partial pressure given by Cameron's formula for this partial density. Inside the core the electron partial pressure is constant. The radius R_c of the boundary of the core (at which $\rho = 3.4 \times 10^{11}$) and the mass M_c contained inside the core are given in Table 8. As was to be expected, $R_n \approx R_c$ and $M_n \approx M_c$ for $\rho_c \gtrsim 10^{14} \gg 3.4 \times 10^{11}$. The minimum value of about $0.03 M_\odot$ for M_n (or M_c) occurs for $R_n \sim 2 \times 10^{-5} R_\odot$ and ρ_c slightly less than ordinary nuclear density (2.26×10^{14} instead of 4×10^{14}), when the attractive nuclear forces are appreciable but the effect of the repulsive short-range forces not yet very marked.

Outside the neutron core, $\rho \leq 3.4 \times 10^{11}$, we have used the pressure formula of Paper I for "equilibrium chemical composition," just as for the models in Table 4. The pressure and density are continuous across the core boundary. The total radius R and mass M of these models with an envelope of ions and electrons are given in the last two

rows of Table 8. Even for the first model in the table, the density at the core boundary is only about $0.01 \rho_c$, and one might have expected the envelope to be unimportant. However, this is not the case at all. The radius and mass of the first few models are very much greater than those of the neutron core and are of the same order of magnitude, $R \sim 10^{-3} R_\odot$, $M \sim 0.7 M_\odot$, as for the last model in Table 4 for $\rho_c \sim 3 \times 10^{11}$. Only for $\rho_c > 3.5 \times 10^{14}$ is the effect of the envelope on the mass small (and for $\rho_c > 5 \times 10^4$ the effect on the radius). The radius and mass decrease extremely rapidly with increasing central density for $\rho_c \sim 3.4 \times 10^{14}$. The density $\rho(r)$ at radial distance r is plotted in

TABLE 8
MODELS FOR NEUTRON STARS WITH ELECTRONS NEGLECTED (R_n, M_n) AND COMPLETE
MODELS (R, M) FOR NEUTRON STARS WITH ENVELOPE CONTAINING IONS AND
ELECTRONS AND PURE NEUTRON CORE (R_c, M_c)

	$10^{-14} \rho_c$								
	0.3	1.0	2.6	3.3	3.42	3.44	3.5	4.0	6.0
$10^4 R_n/R_\odot$	0.33	0.31	0.21	0.13	0.12	0.12	0.12	0.11	0.11
$10 M_n/M_\odot$	0.48	0.45	0.29	0.42	0.46	0.47	0.50	0.75	2.71
$10^4 R_c/R_\odot$	0.25	0.23	0.16	0.11	0.11	0.11	0.11	0.10	0.11
$10 M_c/M_\odot$	0.43	0.41	0.28	0.42	0.46	0.47	0.497	0.750	2.71
$10^4 R/R_\odot$	12.6	12.8	12.8	40.6	88	6.6	1.5	0.25	0.14
$10 M/M_\odot$	6.6	6.8	7.4	8.2	1.1	0.49	0.505	0.752	2.71

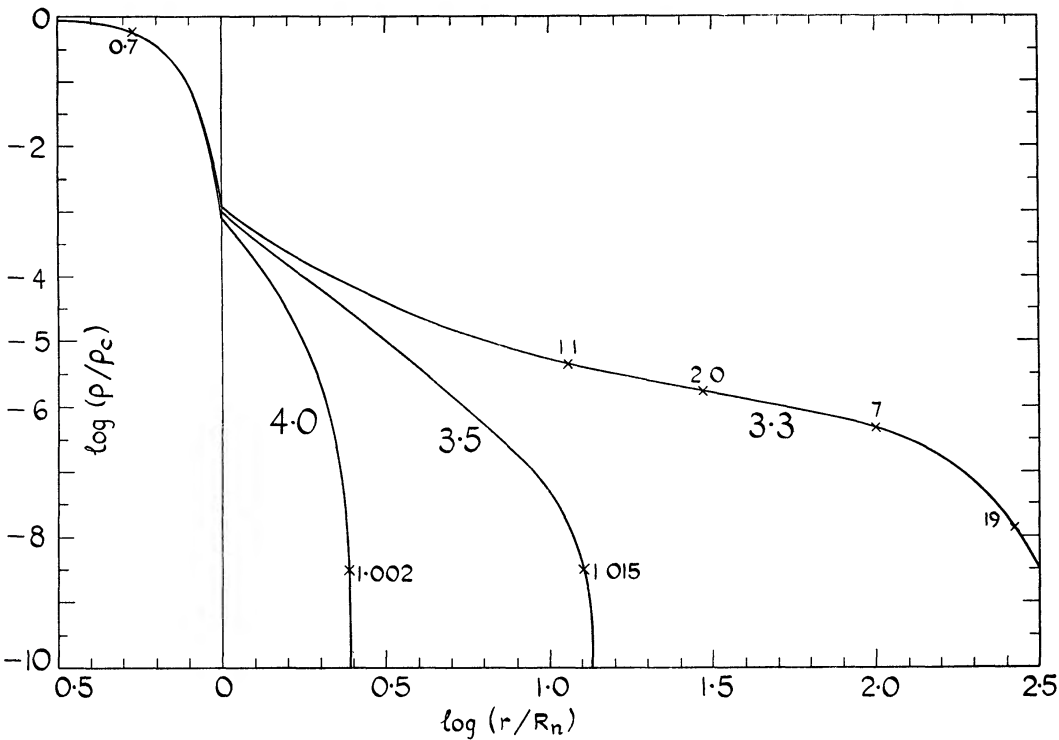


FIG. 4—Density ρ (in units of central density ρ_c) as a function of radial distance r (in units of R_n , the radius of the neutron core) for neutron stars. The curves are labeled by the value of ρ_c in units of 10^{14} gm/cc. The small numbers near the crosses give M_r in units of M_c , the mass of the neutron core.

Figure 4 for three values of ρ_c , showing a very marked decrease in slope outside the core boundary for the lower values of ρ_c .

This unusual behavior of a stellar envelope can be understood as follows: in equation (2) let $f(r) \equiv GM(r)/r^2$, and a dimensional argument for the interior of the neutron core leads to the order-of-magnitude relation

$$R_c \sim \left(\frac{P}{\rho} \right)_{\text{int}} f^{-1}(R_c), \quad (6)$$

where $(P/\rho)_{\text{int}}$ is the ratio of pressure to density in the deep interior of the core, say at $\rho_{\text{int}} \sim 0.3 \rho_c$ or $0.5 \rho_c$. Let $l(r)$ be the "scale height" at radial distance r , defined by $dP/P = -dr/l(r)$, so that

$$l(r) = \frac{P(r)}{\rho(r)} f^{-1}(r). \quad (7)$$

In the neighborhood of the core boundary, $f(r)$ is a slowly varying function and $\rho \ll \rho_{\text{int}}$. Under usual circumstances, P/ρ is an increasing function of ρ (as $\rho^{2/3}$ for a non-relativistic Fermi gas and $\rho^{1/3}$ for a relativistic gas), and a comparison of equations (6) and (7) shows that $l(r) \ll R_c$, i.e., that the envelope has a small thickness. However, this is not necessarily the case for our models, since the partial pressure of neutrons is relatively low at densities below nuclear density. The pressure-density ratio (in arbitrary units) is given in the accompanying table. Thus, for $\rho_{\text{int}} \lesssim 10^{14}$ we have $l(R_c) \gtrsim R_c$; the

	ρ								
	10^9	10^{10}	3.4×10^{11}	10^{12}	10^{13}	10^{14}	2.6×10^{14}	4×10^{14}	6×10^{14}
P/ρ	0.22	0.41	1	0.46	0.66	0.66	1.7	5.1	14

pressure falls off reasonably slowly outside the neutron core; $f(r)$ decreases with $r \gg R_c$; $l(r)$ increases even further and a very extended envelope is obtained. If, on the other hand, $l(R_c)/R_c$ is sufficiently small (for slightly larger ρ_{int}), then the density falls sufficiently rapidly outside the core that P/ρ decreases more rapidly than $f(r)$, $l(r)$ decreases with increasing r , and a thin envelope with a sharp boundary is obtained, as in most stellar models.

In the critical region of $\rho_c \sim 3.4 \times 10^{14}$ our models are rather unreliable. It is not clear whether the increase in R and M with ρ_c up to about 3.4×10^{14} of our models is real. It is certain, however, that R and M are much larger than R_c and M_c up to a critical density of this order and then decrease very rapidly. A minimum mass M of the order of $0.05 M_\odot$ must then occur as soon as ρ_c is sufficient for the envelope to contain little mass (compared with a minimum of about $0.03 M_\odot$ for M_n).

To summarize the results of this paper for $M_0(\rho_c)$, the mass of a model star at equilibrium at zero temperature as a function of central density ρ_c : $M_0(\rho_c)$ has a maximum value in the range of 1.0 – $1.4 M_\odot$ (depending on chemical composition) for $\rho_c \sim 10^9$ – 10^{10} . For larger ρ_c the value of $M_0(\rho_c)$ decreases slowly up to $\rho_c \sim 3 \times 10^{14}$ (the secondary maximum of about $0.8 M_\odot$ at $\rho_c \sim 3.3 \times 10^{14}$ in Table 8 is probably spurious and in any case not very important), then decreases very rapidly to a minimum of about $0.05 M_\odot$ at $\rho_c \sim 3.5 \times 10^{14}$ and then increases again fairly rapidly ($M_0 = 1.0 M_\odot$ at $\rho_c \sim 1.2 \times 10^{15}$).

The function $M_0(\rho_c)$ may be of importance for theories on supernovae explosions of stars of relatively low initial mass (see also Hoyle and Fowler 1960). We have seen that a star of mass between 1.0 and slightly above $1.4 M_\odot$ may be able to contract to high

densities ($\rho_c \sim 10^9\text{--}10^{10}$) at relatively low temperatures. Since $M_0(\rho_c)$ is now a decreasing function of ρ_c , the star can contract further. In an adiabatic contraction at constant mass, in fact, a reasonable fraction of the gravitational energy would be converted into kinetic energy. Furthermore, even a star whose mass decreased with time could keep on contracting as long as its mass at any time was larger than $M_0(\rho_c)$ for the appropriate density at this time. Since the minimum value of $M_0(\rho_c)$ is much smaller ($\sim 0.05 M_\odot$) than the initial mass ($\sim 1 M_\odot$) of the actual star, an appreciable fraction of the initial mass could be shed into an exploding outer shell without stopping the contraction of the inner core of the star. Since $M_0(\rho_c)$ increases again with increasing ρ_c near nuclear density, the contraction of the remaining stellar core must finally cease when $M_0(\rho_c)$ approaches the mass of this core. The stable neutron star remaining must have $\rho_c > 3.5 \times 10^{14}$ (as well as $M > 0.05 M_\odot$), and for these high-density stars the envelopes discussed earlier in this section are relatively unimportant. For cooled-down stable neutron stars the models (without envelopes) of Cameron (1959) should then be reliable.

One of us (E. E. S.) is indebted to the Department of Theoretical Physics, Cambridge University (England), for hospitality and to the U.S. National Science Foundation and Churchill College, Cambridge for Fellowships.

REFERENCES

- Aller, L. H. 1959, *Mém. Soc. R. Sci. Liège*, **3**, 41.
 Auluck, F. C., and Mathur, C. S. 1959, *Zs. f. Ap.*, **48**, 28.
 Cameron, A. G. W. 1959, *Ap. J.*, **130**, 884.
 Chandrasekhar, S. 1935, *M.N.*, **95**, 207.
 ———. 1939, *An Introduction to the Study of Stellar Structure* (Chicago: University of Chicago Press).
 Cox, J. P., and Giuli, R. T. 1961, *Ap. J.*, **133**, 755.
 Cox, J. P., and Salpeter, E. E. 1961, *Ap. J.*, **133**, 764.
 Gill, S. 1951, *Proc. Cambridge Phil. Soc.*, **47**, 96.
 Hoyle, F., and Fowler, W. A. 1960, *Ap. J.*, **132**, 565.
 Kothari, D. S. 1938, *Proc. R. Soc., London A*, **165**, 486.
 Salpeter, E. E. 1960, *Ann. Phys.*, **11**, 393.
 ———. 1961, *Ap. J.* (preceding paper).
 Schatzman, E. 1947, *Ann. d'ap.*, **10**, 19.
 ———. 1958, *White Dwarfs* (New York: Interscience Publishers).
 Singh, R. P. 1957, *Ap. J.*, **126**, 213.
 Singh, R. P., and Goel, N. S. 1960, *Zs. f. Ap.*, **50**, 269.